

MOL#58768

**Context-dependent pharmacology exhibited by negative allosteric modulators of  
metabotropic glutamate receptor 7**

Colleen M. Niswender, Kari A. Johnson, Nicole R. Miller, Jennifer E. Ayala, Qingwei Luo,  
Richard Williams, Samir Saleh, Darren Orton, C. David Weaver, P. Jeffrey Conn

Department of Pharmacology and Vanderbilt Program in Drug Discovery (C.M.N., K.A.J.,  
N.R.M., J.E.A., Q.L., R.W., C.D.W., P.J.C.), Vanderbilt Institute of Chemical Biology (S.S.,  
D.O., C.D.W.), Department of Chemistry (D.O.), Vanderbilt University, Nashville, TN 37232

MOL#58768

Running title: Context-dependent pharmacology of mGluR7 antagonists

Colleen M. Niswender  
1215 MRB IV  
Department of Pharmacology, Vanderbilt University  
Nashville, TN 37232  
615-343-4303  
615-936-6833 (fax)  
[colleen.niswender@vanderbilt.edu](mailto:colleen.niswender@vanderbilt.edu)

Number of text pages: 31

Number of tables: 0

Number of figures: 8

Number of references: 31

Number of words:

Abstract: 247

Introduction: 841

Discussion: 1239

Nonstandard abbreviations: GPCR, G protein coupled receptor; GIRK, G protein-regulated Inwardly Rectifying K (potassium) channel; mGluR, metabotropic glutamate receptor; HEK, human embryonic kidney; DMSO, Dimethylsulfoxide; L-AP4, L-(+)-Amino-4-phosphonobutyric acid; LY 341495, (2*S*)-2-Amino-2-[(1*S*,2*S*)-2-carboxycycloprop-1-yl]-3-(xanth-9-yl) propanoic acid; MMPIP, 6-(4-Methoxyphenyl)-5-methyl-3-(4-pyridinyl)-isoxazolo[4,5-*c*]pyridin-4(5*H*)-one; AMN082, N,N'-Dibenzhydrylethane-1,2-diamine dihydrochloride

MOL#58768

## Abstract

Phenotypic studies of mice lacking metabotropic glutamate receptor subtype 7 (mGluR7) suggest that antagonists of this receptor may be promising for the treatment of CNS disorders such as anxiety and depression. Suzuki et al. (Suzuki et al., 2007) recently reported the *in vitro* characterization of a novel mGluR7 antagonist called MMPIP, which noncompetitively inhibited the activity of orthosteric and allosteric agonists at mGluR7. As reported by Suzuki et al., we describe that MMPIP acts as a noncompetitive antagonist in calcium mobilization assays in cells co-expressing mGluR7 and the promiscuous G protein  $G_{\alpha 15}$ . Assessment of the activity of a small library of MMPIP-derived compounds using this assay reveals that, despite similar potencies, compounds exhibit differences in negative cooperativity for agonist-mediated calcium mobilization. Examination of the inhibitory activity of MMPIP and analogs using endogenous  $G_{i/o}$ -coupled assay readouts indicates that the pharmacology of these ligands appears to be context-dependent and MMPIP exhibits differences in negative cooperativity in certain cellular backgrounds. Electrophysiological studies reveal that, in contrast to the orthosteric antagonist LY341495, MMPIP is unable to block agonist-mediated responses at the Schaffer collateral-CA1 synapse, a location at which neurotransmission has been shown to be modulated by mGluR7 activity. Thus, MMPIP and related compounds differentially inhibit coupling of mGluR7 in different cellular backgrounds and may not antagonize coupling of this receptor to native  $G_{i/o}$  signaling pathways in all cellular contexts. The pharmacology of this compound represents a striking example of the potential for context-dependent blockade of receptor responses by negative allosteric modulators.

MOL#58768

The G protein-coupled receptors (GPCRs) play critical roles in regulating a broad range of signaling pathways within virtually every organ system (George et al., 2002) and are the targets of intense discovery efforts for new drug candidates. Despite this concentrated focus, selective ligands do not exist for the large majority of these receptors (Howard et al., 2001). Many GPCRs interact with natural ligands based on complex or highly restricted chemical scaffolds (for example, amino acids, peptides, lipids, etc.), that are not well suited to optimization of selective small molecule reagents. Additionally, high conservation of the orthosteric sites of GPCR subfamilies presents challenges in developing high selectivity for a given receptor subtype. For these reasons, increasing interest has been placed on identifying compounds that interact with GPCRs at allosteric, rather than orthosteric, binding sites to modulate receptor function. Recently, both positive allosteric modulators (PAMs) and negative allosteric modulators (NAMs) have been described for multiple GPCRs that possess high subtype selectivity and are suitable for modulation of receptor function in both *in vitro* and *in vivo* settings (Conn et al., 2009; Gilchrist and Blackmer, 2007; Groebe, 2009).

While allosteric modulators of GPCRs provide potential advantages over traditional orthosteric ligands, these compounds also introduce new layers of complexity into receptor pharmacology. In recent years, there has been a growing appreciation of the ability of a single GPCR to simultaneously regulate multiple signaling pathways (Kenakin, 2005). Furthermore, ligands can stabilize distinct conformational states of GPCRs, activating or inhibiting a discrete subset of the possible cellular behaviors linked to that receptor. The phenomenon by which different ligands can preferentially stabilize discrete receptor conformations and differentially affecting various signaling pathways has been termed “functional selectivity” or “ligand directed

MOL#58768

trafficking of receptor stimulus” (LDTRS) (reviewed in (Leach et al., 2007; Urban et al., 2007)). In addition to the ability of unique ligands to preferentially stabilize specific receptor conformations to affect signaling, the context for receptor expression may also play a critical role in the pharmacology of individual ligands. Differences in the G protein complement or other receptor-interacting proteins within a cell, for example, may engender different receptor conformations or signaling (in the presence or absence of agonist) potentially altering ligand pharmacology.

Since allosteric modulators stabilize different conformational states of GPCRs, it is anticipated that these compounds could engender functionally selective or context-dependent effects in the actions of orthosteric ligands that co-bind to the receptor. There are now examples of differential signaling effects induced by the actions of GPCR PAMs (Zhang et al., 2005) as well as examples of the “probe dependence” of allosteric modulators, i.e., that certain modulators will behave differently in the presence of distinct orthosteric ligands (Kenakin, 2008). NAMs can also theoretically stabilize distinct receptor conformations, preventing orthosteric agonists from activating some but not all signaling pathways or exhibiting differential levels of negative cooperativity on agonist affinity or efficacy (Kenakin, 2005). While functionally selective and context-dependent behavior of compounds introduces potential complexity into ligand development, it is anticipated that this phenomenon will provide exciting opportunities to tailor new drug therapy to specifically affect coupling of GPCRs to some signaling pathways but not others.

Suzuki et al. recently reported the discovery of the compound MMPIP as a highly selective NAM of the metabotropic glutamate receptor subtype 7 (mGluR7) that exhibits intrinsic inverse agonist activity (Nakamura et al., 2009; Suzuki et al., 2007). This compound

MOL#58768

represents a major breakthrough in that it is the first selective antagonist of mGluR7, a receptor which is thought to play critical roles in regulating excitatory synaptic transmission in many regions of the CNS (Ayala et al., 2008; de Rover et al., 2008; Pelkey et al., 2005). We synthesized MMPIP and multiple MMPIP analogs to develop a further understanding of the actions of this compound. Consistent with previous findings (Suzuki et al., 2007), we observed that MMPIP and related compounds blocked mGluR7-mediated increases in intracellular calcium mobilization via a promiscuous G protein. However, MMPIP and its analogs exhibited lower potencies and efficacies as antagonists of mGluR7 coupling to G-protein-coupled inwardly rectifying potassium (GIRK) channels through endogenous cellular G proteins. Activity of MMPIP on coupling of mGluR7 to inhibition of cAMP accumulation in this same cell line was complex; the compound appeared to inhibit constitutive activity of the receptor but did not block the cAMP-inhibition response induced by an orthosteric agonist. MMPIP was further examined using a label-free technology to directly compare mGluR7 responses in distinct cell backgrounds. In these studies, it was clear that MMPIP exhibited different pharmacology depending upon the cell background for expression. Finally, MMPIP did not block effects of an mGluR7 agonist at a glutamatergic synapse in the hippocampus where a role for mGluR7 has previously been established (Ayala et al., 2008). Since regulation of transmission at excitatory synapses is thought to be a major role of mGluR7, these findings suggest that MMPIP may not block many of the predominant effects of mGluR7 *in vivo*. These results suggest that the actions of MMPIP and potentially other GPCR NAMs may be highly specific for modulating signaling pathways in different cellular contexts.

MOL#58768

## Materials and Methods

*Cell lines and cell culture.* BHK cells stably expressing rat mGluR7a were transfected with a pCDNA 3.1+ plasmid encoding Gα15 (Conklin et al., 1993). Cells were grown in Dulbecco's Modified Eagle Medium (DMEM) containing 10% FBS, 20 mM HEPES, 2 mM L-glutamine, 100 mM penicillin/streptomycin, 1X non-essential amino acids, 1 μM methotrexate, and 400 μg/ml G418 (Mediatech, Inc., Herndon, VA) at 37°C in the presence of 5% CO<sub>2</sub>. Rat mGluR7a/HEK/GIRK cells were grown in growth medium (45% DMEM, 45% F-12, 10% FBS, 20 mM HEPES, 2 mM L-glutamine, 100 mM penicillin/streptomycin, non-essential amino acids, 700 μg/ml G418, and 0.6 μg/ml puromycin) at 37°C in the presence of 5% CO<sub>2</sub>. For both cell lines, cells were plated for assays in Assay Medium (DMEM, 10% dialyzed fetal bovine serum, 20 mM HEPES, 1 mM sodium pyruvate). All cell culture reagents were purchased from Invitrogen (Carlsbad, CA) unless otherwise noted.

*Calcium assays.* One day prior to assay, cells were plated at 30,000 cells/well in a black-wall, clear-bottom 384 well plate (Greiner) in glutamine-free medium, and subjected to heat shock at 42°C for 2.5 hours. Cells were incubated at 37°C, 5% CO<sub>2</sub>, overnight. The following day, cells were incubated for one hour at room temperature with 20 μl of 3 μM Fluo-4, AM, prepared as a 2.3 mM stock in DMSO, mixed in a 1:1 ratio with 10% (w/v) pluronic acid F-127 (Invitrogen, Carlsbad, CA), and diluted in Calcium Assay Buffer (Hank's Balanced Salt Solution, 20 mM HEPES, 2.5 mM probenecid). Dye was then replaced with 20 μl Calcium Assay Buffer. MMPIP-derived test compounds and the group III mGluR agonist L-AP4 were prepared at 2.5X or 5X their final concentrations, respectively, in Calcium Assay Buffer. After initial fluorescence readings in a Hamamatsu FDSS6000 (excitation 470 +/-20 nm, emission

MOL#58768

540 $\pm$ 30 nm), 20  $\mu$ l of test compound was added to cells and fluorescence was measured every 24 s for 30 min. 10  $\mu$ l of vehicle or agonist was then added and fluorescence was measured every second for 2 minutes. Raw data were exported to Microsoft Excel and the maximum fluorescence reading for each trace was measured. Concentration-response curves were integrated and fit using a four-parameter logistic equation in GraphPad Prism (GraphPad Software, Inc., La Jolla, CA).

*Thallium flux assays.* Thallium flux assays for mGluR7, 4 and 8 were performed as described in Niswender et al., (2008) using a Hamamatsu FDSS6000. Briefly, cells were plated at 15,000 cells/well on poly-D-lysine coated 384 well plates (Greiner Bio-One, Monroe, NC) in Assay Medium (Niswender et al., 2008) and the following day the medium was replaced with 20  $\mu$ l of either 1.7  $\mu$ M BTC, AM or 0.33  $\mu$ M Fluo Zn<sup>2+</sup> (FluxOr, Invitrogen) (dyes were pre-mixed 1:1 with 10% pluronic acid 127 and then dissolved in Assay Buffer (Hank's Balanced Salt Solution, 20 mM HEPES Assay Buffer). Cells were incubated with dye for 45 minutes and the dye was removed and replaced with 20  $\mu$ l of Assay Buffer. Baseline fluorescence readings were taken for 3 seconds, 20  $\mu$ l of 2.5x antagonist was added, and fluorescence was measured every 2 seconds for 5 minutes. 10  $\mu$ l of L-AP4 or glutamate was then added and fluorescence was measured for an additional 2 minutes. Fluorescence traces were analyzed by calculating the slope of the change in fluorescence from 10 to 20 seconds after agonist/thallium addition. In full-concentration-response curve experiments of MMPIP, nonspecific effects induced by MMPIP were apparent from parallel experiments with mGluR4, mGluR8, and M4 muscarinic receptor experiments (Figure 3B) and are most likely due to nonspecific inhibition of the GIRK channel or another mechanism mediating background thallium flux in these cells. To correct for these apparent nonspecific effects, concentration-response data were expressed as the percent relative

MOL#58768

EC80 response for each cell line. mGluR7 data were then normalized to the responses obtained in M4-expressing cells by using the following formula:  $100 - (\%EC80 \text{ response obtained in M4-expressing cells} - \%EC80 \text{ response obtained in mGluR7-expressing cells})$ . M4 was chosen as it is an unrelated and family A GPCR, but the data from Figure 3B clearly indicate that mGluR4, 8 and M4-expressing cells showed almost identical levels of inhibition at higher concentrations of MMPIP.

*cAMP inhibition studies.* Cells were plated in a poly-D-lysine coated 96-well plate one day prior to assay. After serum-starving for 2 h, cells were equilibrated using DMEM, 20 mM HEPES, and 0.025% ascorbic acid for 10 minutes at room temperature. Cells were then incubated with 500  $\mu$ M IBMX and antagonist or appropriate vehicle for 30 minutes at 37°C. Forskolin (15  $\mu$ M) and/or increasing concentrations of L-AP4 were then added to cells and incubated at 37°C for an additional 20 minutes. Drug solutions were decanted from cells, and 3% trichloroacetic acid was added for >2 h at 4°C to extract intracellular cAMP. Samples were then incubated with bovine PKA and [<sup>3</sup>H]-cAMP (1 nM) for 2 hours on ice. After harvesting samples onto a GF/B filter plate (Perkin Elmer), samples were counted in a Packard TopCount, and [cAMP] in each sample was determined based on a standard curve of unlabeled cAMP.

*Epic experiments.* Rat mGluR7a/HEK cells were plated at a density of 7,500 cells/well in a 20  $\mu$ l volume in a fibronectin-coated Epic® plate (Corning, Inc., Corning, NY) in Assay Medium. The following day, the medium was removed and cells were incubated in 40  $\mu$ l buffer (Hank's Balanced Salt Solution, 20 mM HEPES, and 0.05-0.5% DMSO depending on the experiment. Plates were incubated for 2 hours at 26°C and a baseline reading was taken every 1.5 minutes for 4.5 minutes. Plates were removed and 10  $\mu$ l of 5x ligand was then added to all wells of the plate simultaneously using the automated liquid handling pipettor of a Hamamatsu FDSS

MOL#58768

6000 and the plate was returned to the Epic® reader. Readings were taken every 1.5 minutes for a total read period of 50 minutes. The magnitude of the wavelength shift recorded by the Epic, measured in picometers, at a particular time point was then extracted from the data trace and the resulting concentration-response curves were fitted to a four -parameter logistic equation using GraphPad Prism 4.0.

*Electrophysiology.* Adult male Sprague Dawley rats (Charles River, Wilmington, MA) were anesthetized with isoflurane, decapitated and the brains were quickly removed and submerged into ice-cold cutting solution (in mM: 110 sucrose, 60 NaCl, 3 KCl, 1.25 NaH<sub>2</sub>PO<sub>4</sub>, 28 NaHCO<sub>3</sub>, 5 glucose, 0.6 (+)-sodium-L-ascorbate, 0.5 CaCl<sub>2</sub>, 7 MgCl<sub>2</sub>) continuously bubbled with 95% O<sub>2</sub>/5% CO<sub>2</sub>. The brains were then hemisected and 400µm transverse slices were made using a vibratome (Leica VT100S). Individual hippocampi were removed from the slice and transferred to a room-temperature mixture containing equal volumes of cutting solution and artificial cerebrospinal fluid (ACSF; in mM: 125 NaCl, 2.5 KCl, 1.25 NaH<sub>2</sub>PO<sub>4</sub>, 25 NaHCO<sub>3</sub>, 25 glucose, 2 CaCl<sub>2</sub>, 1 MgCl<sub>2</sub>) where they were allowed to equilibrate for 30 minutes. The hippocampi were then placed into a holding chamber containing room temperature ACSF continuously bubbled with 95% O<sub>2</sub>/5% CO<sub>2</sub> and allowed to recover for at least 1 hour.

Following recovery, slices were moved to a submersion chamber continuously perfused with oxygenated ACSF at a rate of 1.5 milliliter per minute. ACSF temperature was maintained between 24 and 25°C. Drugs were diluted to the appropriate concentrations in either –DMSO (< 0.1%) plus ACSF or ACSF equilibrated with 95% O<sub>2</sub>/5% CO<sub>2</sub> and applied to the slice through the perfusion medium. Field excitatory postsynaptic potentials (fEPSPs) were evoked at 0.05Hz by placing a bipolar nickel-chromium stimulating electrode in the stratum radiatum near the CA3-CA1 border in order to stimulate the Schaffer collaterals. Baseline intensities that evoked

MOL#58768

half-maximal fEPSPs were chosen for all experiments. Recording electrodes were pulled on a Flaming/Brown micropipette puller (Sutter Instruments) to a resistance of 4-5M $\Omega$ , filled with ACSF and placed in the stratum radiatum of area CA1. Field potentials were recorded using a Warner Instruments PC-505B amplifier (Warner Instruments, Hamden, CT) and analyzed using Clampex 9.2. Sampled data was analyzed off-line using Clampfit 9.2. Three sequential fEPSPs were averaged and their slopes calculated. All fEPSP slopes were normalized to the average slope calculated during the predrug period (percent of predrug).

*Synthesis of MMPIP and analogs.* Synthesis of MMPIP and analogs is described in detail in the Supplemental Chemistry Methods.

*Chemicals.* L-AP4 was purchased from Ascent Scientific and LY341495 and glutamate were purchased from Tocris Bioscience.

MOL#58768

## Results

### **MMPIP and its analogs antagonize responses in rat mGluR7/G $\alpha$ 15 expressing cells.**

We synthesized MMPIP and approximately 40 structurally related analogs to determine the effects of these compounds on mGluR7. Initially, activities of MMPIP-derived compounds were evaluated by determining their effects in Baby Hamster Kidney (BHK) cells co-expressing mGluR7a and the promiscuous G protein G $\alpha$ 15. While mGluR7 is normally thought to couple primarily to G $_{i/o}$  and associated signaling pathways (Saugstad et al., 1994; Wu et al., 1998), this receptor can also couple via G $\alpha$ 15 to induce increases in intracellular calcium mobilization (Corti et al., 1998; Suzuki et al., 2007). Consistent with previous results (Suzuki et al., 2007), MMPIP inhibited calcium mobilization responses induced by the orthosteric mGluR7 agonist L-AP4 with an IC $_{50}$  value of  $70.3 \pm 20.4$  nM (Mean  $\pm$  SEM, Figure 1A). Additionally, L-AP4 concentration-response curves performed in the presence of increasing concentrations of MMPIP revealed a progressive decrease in the maximal L-AP4 response with little change in L-AP4 potency, consistent with a noncompetitive mechanism of action and similar to the findings of Suzuki et al. (Figure 1B; (Suzuki et al., 2007)).

Synthesis and screening of analogs of MMPIP revealed that several compounds exhibited similar inhibitory effects on mGluR7-mediated calcium responses (Figure 2A). Interestingly, concentration response analyses revealed that two analogs of MMPIP examined in more detail, VUSC001 and VUSC027, exhibited similar potencies to that of MMPIP itself ( $79.5 \pm 11.8$  nM and  $49.2 \pm 21$  nM, respectively, Mean  $\pm$  SEM) but exhibited saturable, yet incomplete, levels of antagonism of mGluR7-mediated responses induced by a concentration of agonist eliciting an 80% maximal response (maximal percent blockade, MMPIP,  $100.7 \pm 1.1\%$ ; VUSC001,  $83.2 \pm 4.1\%$ ; VUSC027,  $62.3 \pm 7.0\%$ , Figure 2B). These results are similar to

MOL#58768

previously reported studies with mGluR5 NAMs based on the MPEP scaffold (Rodriguez et al., 2005). This suggests that NAMs in the MMPIP series exhibit a range of abilities to affect agonist-mediated calcium responses induced by L-AP4.

**MMPIP and its analogs are less active in inhibiting mGluR7 regulation of GIRK channels compared to mGluR7-induced calcium mobilization.** Chimeric and promiscuous G proteins are often used as surrogate strategies to more easily assess the activity of GPCRs that might be difficult to measure using other techniques or in high throughput format. mGluR7 is not thought to couple to  $G\alpha_{15}$  in native systems, however, but has been shown to couple to endogenous  $G_{i/o}$  G proteins within different cellular backgrounds, including neurons, to induce downstream responses (Lafon-Cazal et al., 1999; Saugstad et al., 1994; Saugstad et al., 1996; Wu et al., 1998). We recently developed a multiwell plate assay to assess mGluR7-mediated  $G_{i/o}$ -dependent responses (Niswender et al., 2008). This assay is based on the ability of  $G_{i/o}$  G proteins to interact with ion channels via  $G\beta\gamma$  subunits and measures the flux of the ion thallium through GIRK channels. When analogs of MMPIP were screened using this assay, it was observed that all MMPIP analogs showed weaker activity in inhibiting GIRK responses when compared to their activities in the calcium mobilization assay (Figure 3A versus Figure 2A).

The finding that a single concentration of MMPIP does not completely antagonize the GIRK response at a concentration that completely blocks the calcium mobilization response to mGluR7 activation could be due to a number of factors including differential potencies at inhibiting the two responses, different levels of negative cooperativity, distinct cell backgrounds, or a combination of these. We next performed full concentration-response analyses of MMPIP using mGluR4, mGluR7, mGluR8 and M4 muscarinic receptor-expressing cell lines. High concentrations of MMPIP inhibited thallium flux in multiple cell lines including the unrelated

MOL#58768

M4 muscarinic receptor (Figure 3B), suggesting that high concentrations most likely inhibit GIRK potassium channel activity directly or inhibit other cellular components that contribute to overall thallium flux. After correction for potential nonspecific effects of high MMPIP concentrations as outlined in materials and methods, concentration-response curve analyses of corrected thallium flux traces revealed that MMPIP was ~10 fold less potent in inhibiting mGluR7-induced GIRK activation as compared to inhibition of agonist-mediated calcium mobilization ( $718 \pm 90$  nM versus  $70.3 \pm 20.4$  nM, Mean  $\pm$  S.E.M.; Figure 3C versus Figure 1A). At maximally effective concentrations, MMPIP induced only a  $44.5 \pm 4\%$  inhibition of the EC<sub>80</sub> L-AP4 response. In contrast, previous studies from our laboratory have shown that the orthosteric antagonist LY341495 completely blocks L-AP4-induced responses in the mGluR7 thallium flux assay (Niswender et al., 2008).

Due to the low affinity and efficacy of glutamate at mGluR7, L-AP4 is often used as a surrogate agonist. Additionally, in electrophysiology studies, L-AP4 is commonly used as a selective group III mGluR agonist rather than glutamate as glutamate activates all mGluRs as well as ionotropic receptors and glutamate transporters. As it is well known that the effects of allosteric ligands are highly dependent on the agonist, or “probe” used for receptor activation (discussed in (Leach et al., 2007)), we next determined if the low activity of MMPIP in the thallium flux assay would extend to studies in which glutamate was used as the agonist. In these experiments, glutamate induced approximately 20% of the maximal response induced by L-AP4 (data not shown). When agonist responses in the presence and absence of 1  $\mu$ M MMPIP were normalized for each relative agonist response, the maximal blockade induced by MMPIP was not significantly different for the two agonists (Figure 4A,  $71 \pm 3.8\%$  percent inhibition, L-AP4, Figure 4B,  $67.7 \pm 6.8\%$  inhibition, glutamate (Mean  $\pm$  SEM). These results suggest that the

MOL#58768

reduced effect of MMPIP in inhibiting GIRK activity is independent of the use of L-AP4 or glutamate.

**MMPIP does not block L-AP4 induced inhibition of cAMP accumulation in mGluR7/HEK cells.** Differential effects of MMPIP on mGluR7-mediated calcium mobilization versus modulation of GIRK suggest that MMPIP and related compounds differentially modulate mGluR7 depending on the signaling pathway or cellular context in which responses are measured. We next decided to focus on study of the mGluR7/HEK cell line used for the thallium flux experiments. If MMPIP was selective in its ability to block specific signaling pathways, assessing different signaling events in the same cell background was critical to define this as the mechanism. If the blockade induced by MMPIP was context-dependent, in contrast, we would predict that MMPIP would exhibit similar pharmacology in blocking various mGluR7/HEK cell responses which might differ globally from responses seen in cell background such as BHK cells.

The GIRK assay measures the readout downstream of the  $G\beta\gamma$  subunits of the G protein, suggesting that it was formally possible that MMPIP exhibited differential ability to block these responses versus those modulated by the  $G\alpha$  subunits of the heterotrimeric G protein. To further evaluate effects of MMPIP on another response that is mediated by endogenous  $G_{i/o}$  and to assess the ability of the compound to block a  $G\alpha$ -mediated response, we performed studies of effects of MMPIP on mGluR7-mediated inhibition of cAMP accumulation in mGluR7/HEK cells. As previously reported (Suzuki et al., 2007), MMPIP increased cAMP accumulation when added in the absence of L-AP4 (Figure 5A;  $EC_{50}$ ,  $690\pm 130$  nM). This effect of MMPIP on basal cAMP accumulation made it difficult to interpret the level of blockade induced by a single concentration of L-AP4 (data not shown). For this reason, we performed full concentration-

MOL#58768

response analyses of L-AP4 in the presence and absence of 1  $\mu$ M MMPIP, a concentration that was maximally effective in calcium mobilization assays. MMPIP induced a large increase in cAMP levels alone but did not significantly block L-AP4-induced inhibition of cAMP accumulation (Figure 5B). In contrast, the orthosteric antagonist LY341495 completely blocked L-AP4-induced inhibition of cAMP accumulation with no change in forskolin-stimulated cAMP levels alone (Figure 5B). These data suggested that, compared to responses in BHK cells, MMPIP demonstrated reduced negative cooperativity in blocking two pathways when mGluR7 was expressed in HEK cells, one downstream of G $\beta\gamma$  subunits and one downstream of G $\alpha$  subunits. These data provided further evidence for context-dependence of MMPIP action on mGluR7.

**MMPIP exhibits context-dependent, saturable, effects on mGluR7 activity using an additional phenotypic assay of mGluR7 function.** One difference between the effects measured between BHK cells and HEK cells is the nature of the G protein used for signal transduction. For example, it is possible that MMPIP may be more effective at inhibiting responses that are mediated by coupling of mGluR7 to a promiscuous G protein than to endogenous G $_{i/o}$ . In contrast, MMPIP effects may be dependent upon the cell background in which the receptor is expressed. To more directly compare the effects of MMPIP on responses to mGluR7 activation between cellular backgrounds, we measured mGluR7 activity using a novel phenotypic assay of GPCR function (Epic<sup>TM</sup>, Corning Incorporated). This technique relies on plating cells expressing the receptor of interest onto a plate in which individual wells contain a resonance waveguide grating. Initial baseline readings are taken by illuminating the plate with a broadband light source and measuring the wavelength of the refracted light. After cell stimulation, mass redistribution of intracellular components occurs, resulting in a shift in the

MOL#58768

refracted wavelength. Responses are measured as a picometer wavelength shift from the initial recorded wavelength and can occur in either a positive or negative direction. Rather than reflecting effects of receptor activation on a single signaling pathway, this assay is thought to provide a measure of effects on a composite of different signaling responses to a GPCR ligand, although certain pathways presumably dominate the measured kinetic trace. L-AP4 induced concentration-dependent wavelength shifts in both mGluR7/BHK/G $\alpha$ 15 and mGluR7/HEK cells using the Epic<sup>TM</sup> system (Figure 6A, effects of L-AP4 alone in mGluR7/HEK cells are shown). L-AP4 was equipotent in inducing Epic<sup>TM</sup> responses in mGluR7 BHK and mGluR7/HEK cells (Figure 7A mGluR7/BHK, L-AP4 EC<sub>50</sub>, 177  $\pm$  51  $\mu$ M; 7B, mGluR7/HEK, L-AP4 EC<sub>50</sub>, 195  $\pm$  60  $\mu$ M, Mean  $\pm$  SEM). These L-AP4 responses were blocked in both cell lines by pertussis toxin (data not shown), a compound which prevents signaling through G<sub>i/o</sub> proteins. This suggests that the L-AP4 responses in both cell lines using the Epic<sup>TM</sup> readout are mediated by G<sub>i/o</sub> proteins rather than, for the BHK cell line, G $\alpha$ 15; this might be expected as G $\alpha$ 15 couples weakly to mGluR7 (Corti et al., 1998) and our calcium responses in this cell line are detectable but extremely small compared to native or overexpressed Gq coupled receptors (data not shown). As with the cAMP measurements, MMPIP clearly induced responses alone; these responses were concentration-dependent, appeared to be specific to mGluR7 as there was no corresponding response in mGluR4-expressing cells (Figure 7C) and the wavelength shifts were in the opposite direction of those induced by L-AP4 (representative example of traces shown in Figure 6B; resulting concentration-response curve for mGluR7/HEK cells shown as black squares in Figure 7C). Concentration-response curves of L-AP4 in the presence of 1  $\mu$ M MMPIP were, again, very different between the two cell lines, with much more robust inhibition being observed in mGluR7/BHK cells compared to mGluR7/HEK cells (Figure 7A versus 7B). Concentration-

MOL#58768

response curves of MMPIP in the presence of an EC<sub>80</sub> concentration of L-AP4, when corrected for responses obtained in the presence of the compound alone, again revealed distinct levels of inhibition between the two cell lines (Figure 7D). Importantly, these concentration-response curves were saturable, suggesting that these effects are not due to differences in receptor expression between the two cell lines. A fit of the normalized data revealed that MMPIP blocked responses in mGluR7/HEK cells by  $46.0 \pm 1.8\%$  with a potency of  $156 \pm 28$  nM (Figure 7D; Mean  $\pm$ SEM, n=3). This level of inhibition was remarkably similar to the effect observed in the thallium flux assay when the data were corrected for nonspecific effects ( $44.5 \pm 4\%$ ). In contrast, in mGluR7/BHK cells, MMPIP was exhibited a potency similar to that observed in the calcium assay as well as increased maximal blockade compared to mGluR7/HEK cells ( $75.2 \pm 3.3\%$  blockade,  $50 \pm 15$  nM; Mean $\pm$ SEM, n=3).

**MMPIP is ineffective at blocking L-AP4-mediated reductions of synaptic transmission at the Schaffer collateral-CA1 synapse.** In its native environment, mGluR7 is predominantly expressed in presynaptic terminals of excitatory glutamatergic synapses (Shigemoto et al., 1997) where it is thought to serve as an autoreceptor to inhibit glutamate release. The actions of group III mGluR activation have been most rigorously evaluated at a glutamatergic synapse in the hippocampal formation termed the Schaffer collateral-CA1 (SC-CA1) synapse (Ayala et al., 2008; Baskys and Malenka, 1991; Gereau and Conn, 1995). Activation of mGluR7 with L-AP4 reduces evoked excitatory postsynaptic potentials (EPSPs) at this synapse and evidence suggests that there is no contribution of mGluR4 or mGluR8 to the response to L-AP4 at the SC-CA1 synapse in adult animals (Ayala et al., 2008). To assess the effect of MMPIP on mGluR7 activity in a native system, we determined the effects of this compound on L-AP4-induced modulation of transmission at the SC-CA1 synapse. Consistent

MOL#58768

with previous reports, L-AP4 (400  $\mu$ M) reduced the initial slope of field excitatory postsynaptic potentials (fEPSPs) recorded at the SC-CA1 synapse. The concentration of L-AP4 used was chosen based on L-AP4 concentration-response curves showing that this concentration elicits a robust but submaximal response. Consistent with our previous reports, (Ayala et al., 2008) the orthosteric antagonist LY341495 significantly blocked L-AP4 mediated reductions in neurotransmission (Figure 8A and 8C). In contrast, MMPIP, at a 10  $\mu$ M concentration (approximately 100x higher than the  $IC_{50}$  in *in vitro* calcium assay experiments), was not effective in blocking effects of L-AP4 on transmission at this synapse (Figure 8B and 8D). Overall, the combination of *in vitro* pharmacology and electrophysiology results suggest that MMPIP exhibits differential degrees of negative cooperativity in different cellular contexts and is ineffective at antagonizing mGluR7 activity at a central glutamatergic synapse that is thought to reflect one of the major physiological roles of this GPCR in the CNS.

MOL#58768

## Discussion

Until recently, the focus of most GPCR ligand discovery programs has been on the development of orthosteric ligands. Recently, allosteric compounds have begun to emerge as a potentially useful strategy by which to modulate receptor function and these ligands possess several advantages (discussed in (Conn et al., 2009)). For example, many orthosteric ligands are based on chemical scaffolds that are difficult to optimize as drug candidates with ideal pharmacokinetic properties; in contrast, allosteric ligands are often amenable to chemical optimization. Furthermore, allosteric ligands often exhibit a high degree of selectivity for a particular receptor over closely related subtypes. Additionally, PAMs, which often have no effect on their own but instead act by potentiating the effects of the orthosteric ligand, have the ability to maintain the temporal and spatial activity of the endogenous agonist. While potential advantages of maintaining activity-dependence are largely theoretical, examples are beginning to emerge in which PAMs provide more physiologically appropriate increases in receptor function than is seen with traditional agonists (Ayala et al., 2008).

As the development of allosteric ligands has grown, so has the appreciation of their underlying pharmacology. As these compounds bind to alternate sites on a GPCR compared to the endogenous ligand, it might be expected that they could place the receptor in a unique structural conformation that might not be achieved, or at least favored, in their absence. This could result in preferential regulation of certain pathways in the presence of an allosteric ligand. For example, the allosteric modulator CPPHA exhibits differential effects on calcium mobilization and ERK1/2 phosphorylation downstream of mGluR5 activation in cultured cortical astrocytes (Zhang et al., 2005). As an example of complex pharmacology induced by NAMs, 1-(4-ethoxyphenyl)-5-methoxy-2-methylindole-3-carboxylic acid is an allosteric modulator of the

MOL#58768

chemo-attractant-receptor-homologous molecule, CRTH2, on T helper (Th)2 cells. This compound has been shown to be inactive against prostaglandin D<sub>2</sub>-induced G protein-linked pathways but acts as a potent antagonist of G protein-independent,  $\beta$ -arrestin coupling to the same receptor (Mathiesen et al., 2005).

The compound presented here, MMPIP, may best be referred to as exhibiting “context-dependent” pharmacology. MMPIP was discovered using a BHK cell line in which the promiscuous G protein G $\alpha$ 15 was co-expressed to induce calcium mobilization (Suzuki et al., 2007). We generated an analogous cell line and replicated the findings of Suzuki et al., including the observation that MMPIP seemed to act via a noncompetitive mechanism of action. However, further analysis of the effects of MMPIP and analogs revealed activities consistent with a range of negative cooperativities induced by members of this structural class in the calcium mobilization assay. Movement to a different cell background revealed that MMPIP showed weaker potency and efficacy in inhibiting mGluR7 modulation of GIRK potassium channels and was essentially devoid of antagonist activity in blocking mGluR7-mediated inhibition of cAMP accumulation in contrast to its apparent inverse agonist effects. These experiments were designed to assess either G $\beta\gamma$  or G $\alpha$ -mediated signaling arms of G<sub>i/o</sub> proteins and are consistent with MMPIP showing reduced negative cooperativity in the HEK cell, compared to the BHK cell, background. Finally, MMPIP exhibited differential but saturable abilities to block L-AP4-induced signals in different cell lines assessed using Epic<sup>TM</sup> technology, an assay which can be used to compare integrated receptor signaling events in different cellular backgrounds. Preliminary results suggest that the differential effects observed were not due to the presence of G $\alpha$ 15 in the BHK cell line as the response was blocked by the G<sub>i/o</sub> inactivator pertussis toxin (data not shown). We would note, however, that the blockade in the BHK cell line does saturate

MOL#58768

at approximately 75% blockade versus the 100% blockade seen in calcium responses. Therefore, there may still be distinctions in signaling that depend upon the G protein mediating the response with potential distinctions in signaling between  $G\alpha_{15}$  (for calcium mobilization) and  $G_{i/o}$  (for Epic<sup>TM</sup>). Additionally, the  $G_{i/o}$  complement between HEK and BHK cells may differ, which could also contribute to the differences seen between the two cell lines.

In contrast to LY341495, MMPIP did not block mGluR7-mediated depression of transmission at the SC-CA1 synapse. While this does not necessarily imply that MMPIP will be ineffective at blocking all mGluR7 responses in native systems, previous studies suggest that the predominant role of mGluR7 in the CNS is to act as an autoreceptor involved in reducing transmission at glutamatergic synapses via  $G_{i/o}$ -mediated signaling. Thus, it is possible that MMPIP will have relatively little effect on this important response to mGluR7 at other central synapses. MMPIP exhibited similar effects on L-AP4 versus glutamate-mediated thallium flux, suggesting that MMPIP will also exhibit low levels of negative cooperativity in blocking certain glutamate-mediated effects *in vivo*. In future studies it will be important to further evaluate the effects of MMPIP at other synapses and on other responses in CNS preparations. Interestingly, we and others have observed similar context-dependent effects with the allosteric mGluR7 agonist, AMN082. AMN082 appears to be capable of activating mGluR7 when measured in some pathways and cell backgrounds but not others ((Ayala et al., 2008; Suzuki et al., 2007), CMN, unpublished observations). Notably, AMN082 is similar to MMPIP in that this compound is without effect at the SC-CA1 synapse (Ayala et al., 2008), further suggesting complexity in mGluR7 ligand pharmacology in terms of both NAMs and allosteric activators.

The finding that the context of expression of mGluR7 plays a critical role in its function and pharmacology is, perhaps, not unexpected based on studies exploring the regulation of

MOL#58768

mGluR7 by intracellular interacting proteins. The mGluR7 C-terminal tail binds to a variety of interacting proteins such as the clustering protein PICK1 (Protein Interacting with C Kinase 1) (Dev et al., 2001; El Far and Betz, 2002). PICK1 also binds Protein Kinase C $\alpha$  (PKC $\alpha$ ), and the three proteins form a complex at the active zones of presynaptic terminals (El Far and Betz, 2002). Additionally, mGluR7a interacts with Ca<sup>2+</sup>/calmodulin, G protein  $\beta\gamma$  subunits, and the protein MacMARKS (macrophage myristoylated alanine rich C kinase substrate) via the C-terminal tail region (Bertaso et al., 2006). It has been hypothesized that this complex signaling system, coupled with the low affinity of mGluR7 for glutamate, may provide a way to ensure that mGluR7 is only activated during periods of intense synaptic activity and allow the receptor to serve as an integrator of multiple presynaptic signaling events, including rises in intracellular calcium.

Bertaso et al. recently described an elegant set of studies in which the mGluR7a-PICK1 interaction was disrupted by employing a viral vector in which the last nine amino acids of the C-terminus of mGluR7 were used as “bait” to compete with full-length receptor-PICK1 binding (Bertaso et al., 2008). Infection of neurons with this construct *in vivo* inhibited mGluR7-PICK1 interactions and led to absence seizures and EEG waveform changes specifically within thalamo-cortical brain regions. Interestingly, mGluR7 modulation effects induced by viral infection appeared to be specific to thalamo-cortical circuits and mGluR7 activity in the hippocampus, as assessed by c-fos immunostaining or EEG recordings, was not affected. These findings suggest that it is possible that protein-protein interactions or the cellular context in which those protein interactions occur may affect mGluR7 activity *in vivo* and raise the intriguing possibility that the pharmacology of ligands interacting with this receptor may be intimately regulated by protein-protein interactions. It will be of interest to further explore these interactions and determine their

MOL#58768

implications for mGluR7-based drug design and development as this receptor is a key target for numerous CNS disorders such as epilepsy and anxiety (Niswender et al., 2005).

MOL#58768

## References

- Ayala JE, Niswender CM, Luo Q, Banko JL and Conn PJ (2008) Group III mGluR regulation of synaptic transmission at the SC-CA1 synapse is developmentally regulated. *Neuropharmacology* **54**(5):804-814.
- Baskys A and Malenka RC (1991) Agonists at metabotropic glutamate receptors presynaptically inhibit EPSCs in neonatal rat hippocampus. *J Physiol* **444**:687-701.
- Bertaso F, Lill Y, Airas JM, Espeut J, Blahos J, Bockaert J, Fagni L, Betz H and El-Far O (2006) MacMARCKS interacts with the metabotropic glutamate receptor type 7 and modulates G protein-mediated constitutive inhibition of calcium channels. *J Neurochem* **99**(1):288-298.
- Bertaso F, Zhang C, Scheschonka A, de Bock F, Fontanaud P, Marin P, Huganir RL, Betz H, Bockaert J, Fagni L and Lerner-Natoli M (2008) PICK1 uncoupling from mGluR7a causes absence-like seizures. *Nat Neurosci* **11**(8):940-948.
- Conn PJ, Christopoulos A and Lindsley CW (2009) Allosteric modulators of GPCRs: a novel approach for the treatment of CNS disorders. *Nat Rev Drug Discov* **8**(1):41-54.
- Corti C, Restituito S, Rimland JM, Brabet I, Corsi M, Pin JP and Ferraguti F (1998) Cloning and characterization of alternative mRNA forms for the rat metabotropic glutamate receptors mGluR7 and mGluR8. *Eur J Neurosci* **10**(12):3629-3641.
- de Rover M, Meye FJ and Ramakers GM (2008) Presynaptic metabotropic glutamate receptors regulate glutamatergic input to dopamine neurons in the ventral tegmental area. *Neuroscience* **154**(4):1318-1323.
- Dev KK, Nakanishi S and Henley JM (2001) Regulation of mglu(7) receptors by proteins that interact with the intracellular C-terminus. *Trends Pharmacol Sci* **22**(7):355-361.
- El Far O and Betz H (2002) G-protein-coupled receptors for neurotransmitter amino acids: C-terminal tails, crowded signalosomes. *Biochem J* **365**(Pt 2):329-336.
- George SR, O'Dowd BF and Lee SP (2002) G-protein-coupled receptor oligomerization and its potential for drug discovery. *Nat Rev Drug Discov* **1**(10):808-820.
- Gereau RW and Conn PJ (1995) Multiple presynaptic metabotropic glutamate receptors modulate excitatory and inhibitory synaptic transmission in hippocampal area CA1. *J Neurosci* **15**(10):6879-6889.
- Gilchrist A and Blackmer T (2007) G-protein-coupled receptor pharmacology: examining the edges between theory and proof. *Curr Opin Drug Discov Devel* **10**(4):446-451.
- Groebe DR (2009) In search of negative allosteric modulators of biological targets. *Drug Discov Today* **14**(1-2):41-49.
- Howard AD, McAllister G, Feighner SD, Liu Q, Nargund RP, Van der Ploeg LH and Patchett AA (2001) Orphan G-protein-coupled receptors and natural ligand discovery. *Trends Pharmacol Sci* **22**(3):132-140.
- Kenakin T (2005) New concepts in drug discovery: collateral efficacy and permissive antagonism. *Nat Rev Drug Discov* **4**(11):919-927.
- Kenakin T (2008) Functional selectivity in GPCR modulator screening. *Comb Chem High Throughput Screen* **11**(5):337-343.
- Lafon-Cazal M, Fagni L, Guiraud MJ, Mary S, Lerner-Natoli M, Pin JP, Shigemoto R and Bockaert J (1999) mGluR7-like metabotropic glutamate receptors inhibit NMDA-

MOL#58768

- mediated excitotoxicity in cultured mouse cerebellar granule neurons. *Eur J Neurosci* **11**(2):663-672.
- Leach K, Sexton PM and Christopoulos A (2007) Allosteric GPCR modulators: taking advantage of permissive receptor pharmacology. *Trends Pharmacol Sci* **28**(8):382-389.
- Mathiesen JM, Ulven T, Martini L, Gerlach LO, Heinemann A and Kostenis E (2005) Identification of indole derivatives exclusively interfering with a G protein-independent signaling pathway of the prostaglandin D2 receptor CRTH2. *Mol Pharmacol* **68**(2):393-402.
- Nakamura M, Kurihara H, Suzuki G, Mitsuya M, Ohkubo M and Ohta H (2009) Isoxazolopyridone derivatives as allosteric metabotropic glutamate receptor 7 antagonists. *Bioorg Med Chem* doi: **10.1016/j.bmcl.2009.11.070**.
- Niswender CM, Johnson KA, Luo Q, Ayala JE, Kim C, Conn PJ and Weaver CD (2008) A novel assay of Gi/o-linked G protein coupled receptor coupling to potassium channels provides new insights into the pharmacology of the group III metabotropic glutamate receptors. *Mol Pharmacol*.
- Niswender CM, Jones CK and Conn PJ (2005) New therapeutic frontiers for metabotropic glutamate receptors. *Curr Top Med Chem* **5**(9):847-857.
- Pelkey KA, Lavezzari G, Racca C, Roche KW and McBain CJ (2005) mGluR7 is a metaplastic switch controlling bidirectional plasticity of feedforward inhibition. *Neuron* **46**(1):89-102.
- Rodriguez AL, Nong Y, Sekaran NK, Alagille D, Tamagnan GD and Conn PJ (2005) A close structural analog of 2-methyl-6-(phenylethynyl)-pyridine acts as a neutral allosteric site ligand on metabotropic glutamate receptor subtype 5 and blocks the effects of multiple allosteric modulators. *Mol Pharmacol* **68**(6):1793-1802.
- Saugstad JA, Kinzie JM, Mulvihill ER, Segerson TP and Westbrook GL (1994) Cloning and expression of a new member of the L-2-amino-4-phosphonobutyric acid-sensitive class of metabotropic glutamate receptors. *Mol Pharmacol* **45**(3):367-372.
- Saugstad JA, Segerson TP and Westbrook GL (1996) Metabotropic glutamate receptors activate G-protein-coupled inwardly rectifying potassium channels in *Xenopus* oocytes. *J Neurosci* **16**(19):5979-5985.
- Shigemoto R, Kinoshita A, Wada E, Nomura S, Ohishi H, Takada M, Flor PJ, Neki A, Abe T, Nakanishi S and Mizuno N (1997) Differential presynaptic localization of metabotropic glutamate receptor subtypes in the rat hippocampus. *J Neurosci* **17**(19):7503-7522.
- Suzuki G, Tsukamoto N, Fushiki H, Kawagishi A, Nakamura M, Kurihara H, Mitsuya M, Ohkubo M and Ohta H (2007) In vitro pharmacological characterization of novel isoxazolopyridone derivatives as allosteric metabotropic glutamate receptor 7 antagonists. *J Pharmacol Exp Ther* **323**(1):147-156.
- Urban JD, Clarke WP, von Zastrow M, Nichols DE, Kobilka B, Weinstein H, Javitch JA, Roth BL, Christopoulos A, Sexton PM, Miller KJ, Spedding M and Mailman RB (2007) Functional selectivity and classical concepts of quantitative pharmacology. *J Pharmacol Exp Ther* **320**(1):1-13.
- Wu S, Wright RA, Rockey PK, Burgett SG, Arnold JS, Rosteck PR, Jr., Johnson BG, Schoepp DD and Belagaje RM (1998) Group III human metabotropic glutamate receptors 4, 7 and 8: molecular cloning, functional expression, and comparison of pharmacological properties in RGT cells. *Brain Res Mol Brain Res* **53**(1-2):88-97.

MOL#58768

Zhang Y, Rodriguez AL and Conn PJ (2005) Allosteric potentiators of metabotropic glutamate receptor subtype 5 have differential effects on different signaling pathways in cortical astrocytes. *J Pharmacol Exp Ther* **315**(3):1212-1219.

MOL#58768

## Footnotes

This work was supported by funding from the NIH [Grants NS053536, NS031373, NS048334] and the Michael J. Fox Foundation. Portions of this work have been presented at the 2007 Society for Neuroscience Meeting, the 2007 American College of Neuropsychopharmacology Meeting, and the 2008 6th International Meeting on Metabotropic Glutamate Receptors. The authors thank Dr. Karen Gregory for comments on the manuscript.

Reprint requests should be sent to:

Colleen M. Niswender

12478C MRB IV

Department of Pharmacology

Vanderbilt Program in Drug Discovery

Vanderbilt University

Nashville, TN 37232

(615) 343-4303 (phone)

Colleen.niswender@vanderbilt.edu

MOL#58768

## Figure Legends

**Figure 1. MMPIP antagonizes responses in mGluR7/BHK/G $\alpha$ 15 cells in a noncompetitive fashion.** A. Cells co-expressing rat mGluR7a and the promiscuous G protein G $\alpha$ 15 were incubated with increasing concentrations of MMPIP prior to the addition of an EC<sub>80</sub> concentration of the group III mGluR agonist L-AP4 and calcium mobilization was measured. EC<sub>50</sub>= 70.3 $\pm$ 20.4 nM. B. L-AP4 concentration-response curves were performed in the presence of increasing concentrations of MMPIP. Values represent Mean  $\pm$  S.E.M. of three independent experiments performed in quadruplicate.

**Figure 2. MMPIP analogs exhibit a range of efficacies for inhibition of mGluR7-mediated calcium mobilization.** A. Compounds were pre-applied to mGluR7a/BHK/G $\alpha$ 15 cells prior to the addition of an EC<sub>80</sub> concentration of L-AP4 and calcium mobilization was measured. B. Selected compounds were assessed in full concentration-response format for inhibition of mGluR7-mediate calcium mobilization. MMPIP data is replotted from Figure 1B for comparison. Potencies were: VUSC001: 79.5 $\pm$ 11.8 nM, VUSC027: 49.2 $\pm$ 21.0 nM. Maximal inhibition values for each compound (calculated the lowest point of the curve fit as determined using a four site logistical equation in GraphPad Prism) were: MMPIP, 100.7 $\pm$ 1.1%, VUSC001: 83.1 $\pm$ 4.1%, VUSC027: 62.3 $\pm$ 7.0%. Values represent Mean  $\pm$  S.E.M. of at least three experiments performed in quadruplicate.

**Figure 3. MMPIP analogs exhibit lower efficacies in thallium flux assays and the potency of MMPIP is lower than in calcium mobilization studies.** A. Compounds were pre-applied to mGluR7a/HEK/GIRK cells prior to the addition of an EC<sub>80</sub> concentration of L-AP4 and thallium flux through the GIRK channel was measured. B. MMPIP concentration-response

MOL#58768

in thallium flux assays using cells expressing mGluR4, mGluR7, mGluR8 and M4 muscarinic receptor. In each case concentration-response curves were applied to cells prior to an appropriate EC80 concentration of either L-AP4 (mGluR4, 7 and 8) or acetylcholine (M4). The potency of MMPIP in these experiments was  $2.0 \pm 0.2 \mu\text{M}$ . C. Corrected concentration-response curve for MMPIP after normalizing for nonspecific effects of the compound on M4/GIRK cells. Methods for this correction are described in the Materials and Methods. Revised potency of MMPIP,  $717 \pm 89 \text{ nM}$ . Values represent Mean  $\pm$  S.E.M. and are an n of three experiments performed in quadruplicate.

**Figure 4. The level of MMPIP blockade is not probe dependent in the GIRK/thallium flux assay.** A  $1 \mu\text{M}$  final concentration of MMPIP was pre-applied prior to the addition of increasing concentrations of L-AP4 (A) or glutamate (B) and thallium flux was measured. The maximal blockade was  $71 \pm 3.8\%$  for L-AP4 (A) and  $67.7 \pm 6.8\%$ , glutamate. Data represent Mean  $\pm$  S.E.M. of 3 independent experiments performed in quadruplicate.

**Figure 5. MMPIP raises basal cAMP levels and fails to effectively block L-AP4-mediated inhibition of cAMP accumulation.** A. MMPIP induced a concentration-dependent increase in cAMP accumulation in mGluR7/HEK cells ( $\text{EC}_{50} = 690 \pm 130 \text{ nM}$ ). B. In contrast to blockade obtained in the presence of  $100 \mu\text{M}$  of the orthosteric antagonist LY341495 (closed circles), a  $1 \mu\text{M}$  concentration of MMPIP (open squares) increased basal cAMP levels but did not effectively block L-AP4 mediated inhibition of cAMP accumulation (compared maximal blockade to curve of L-AP4 alone, closed squares). Data represent Mean  $\pm$  S.E.M. of 3 independent experiments performed in triplicate.

**Figure 6. L-AP4 and MMPIP induce opposing responses in mGluR7/HEK cells using Epic™ technology.** mGluR7/HEK cells were plated into 384 well Epic plates as

MOL#58768

described in Materials and Methods. Increasing concentrations of L-AP4 (A) or MMPIP (B) were applied to cells and Epic<sup>TM</sup> responses were measured.

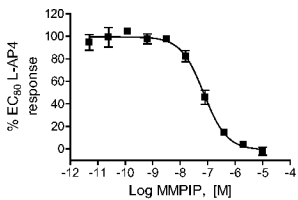
**Figure 7. MMPIP antagonizes L-AP4 responses at mGluR7 with distinct and saturable efficacies in mGluR7/HEK and mGluR7/BHK cells as assessed using Epic<sup>TM</sup> technology.** Increasing concentrations of L-AP4 were added to mGluR7/BHK (A) or mGluR7/HEK (B) cells in the presence (white squares) and absence (black squares) of 1  $\mu$ M MMPIP and the responses, measured as a change in refractive index indicative of cellular mass distribution, were determined. C. Increasing concentrations of MMPIP were incubated with mGluR7/HEK (black squares) or mGluR4/HEK (white squares) cells in the absence of agonist. MMPIP induced decreases in refractive index in cells expressing mGluR7 but not cells expressing mGluR4. D. Increasing concentrations of MMPIP were incubated with mGluR7/BHK (black circles) mGluR7/HEK (white squares) cells in the absence or presence of an EC<sub>80</sub> concentration of L-AP4. Individual responses in the presence of L-AP4 were subtracted by the response induced by MMPIP in the absence of L-AP4. The potency of MMPIP in mGluR7/BHK cells was  $50 \pm 15$  nM and in mGluR7/HEK cells was  $156 \pm 28$  nM. The percent maximal blockade was  $75.2 \pm 3.3\%$  in mGluR7/BHK cells and  $46.0 \pm 1.8\%$  in mGluR7/HEK cells Data for each panel represent Mean  $\pm$  S.E.M. of three independent experiments performed in quadruplicate.

**Figure 8. MMPIP does not block L-AP4-mediated depression of synaptic transmission at the Schaffer collateral-CA1 synapse.** Field excitatory postsynaptic potentials (fEPSPs) were measured at the SC-CA1 synapse in adult rat hippocampus. A. The effect of a submaximal concentration of L-AP4 on fEPSP slope (400  $\mu$ M) over time is shown (dark symbols). This response was significantly blocked by a five minute preincubation with 100  $\mu$ M

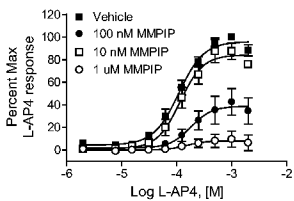
MOL#58768

LY341495 (white symbols). After normalizing for responses across slices, the maximal effect of LY341495 over a five minute period was quantified as shown in figure 8C. (\*p=.0065). B. A five minute preincubation with 10  $\mu$ M MMPIP prior to L-AP4 addition had no significant effect on fEPSP slope; quantified in Figure 8D. Data are from 4-5 slices derived from 2-3 animals.

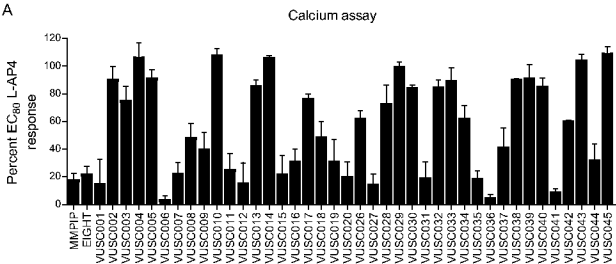
A



B



A



B

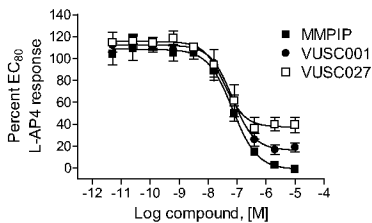


Figure 2.

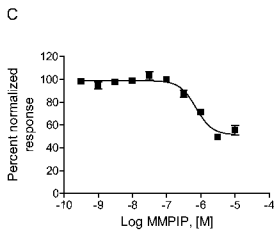
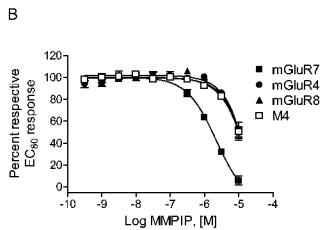
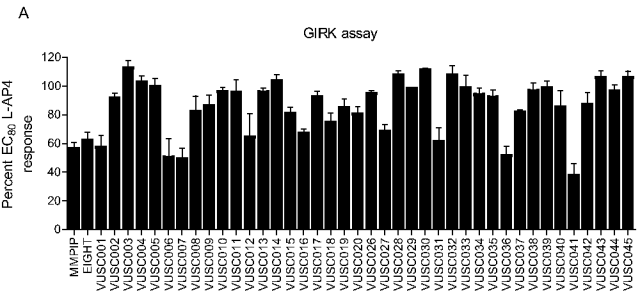
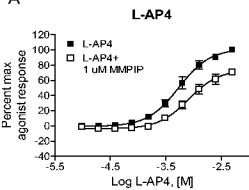


Figure 3.

A



B

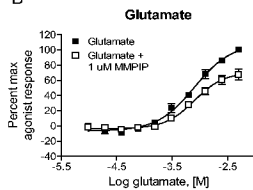


Figure 4.

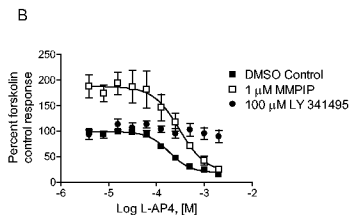
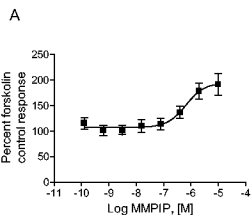
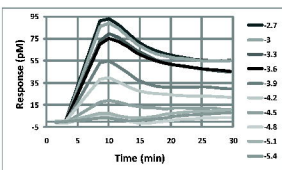
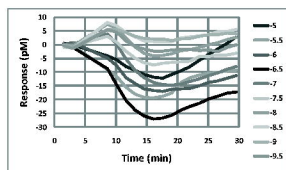


Figure 5.

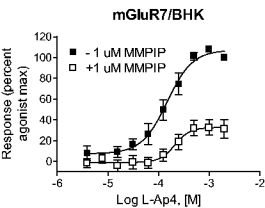
A



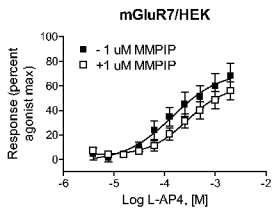
B



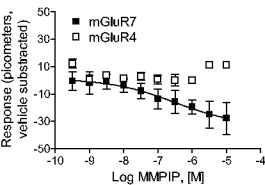
A



B



C



D

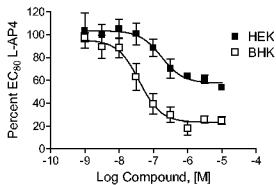
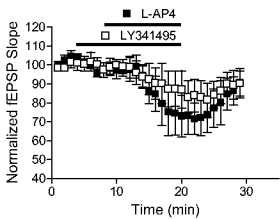
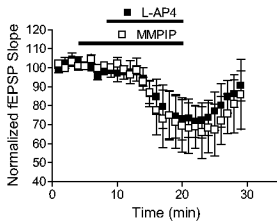


Figure 7.

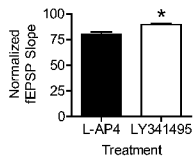
A



B



C



D

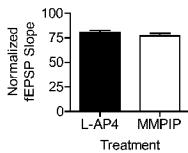


Figure 8.